PAPER • OPEN ACCESS

Anti-bacteria activity of carbon nanotubes grown on trimetallic catalyst

To cite this article: S O Ibrahim *et al* 2018 *Adv. Nat. Sci: Nanosci. Nanotechnol.* **9** 025008

View the article online for updates and enhancements.

Related content

Anti-bacteria activity of carbon nanotubes grown on trimetallic catalyst

S O Ibrahim[1,2]**, A S Abdulkareem**[1,3]**, K U Isah**[1,2]**, U Ahmadu**[2]**, M T Bankole**[1,4] **and I Kariim**[1,3]

[1] Nanotechnology Group, Centre for Biotechnology and Genetic Engineering, Federal University of Technology, Minna, Nigeria
[2] Physics Department, Federal University of Technology, Minna, Nigeria
[3] Chemical Engineering Department, Federal University of Technology, Minna, Nigeria
[4] Chemistry Department, Federal University of Technology, Minna, Nigeria

E-mail: bankole.temitope@futminna.edu.ng

CrossMark

Abstract

Trimetallic Fe-Ni-Co/Al_2O_3 catalyst was prepared using wet impregnation method to produce carbon nanotubes (CNTs) through the method of catalytic chemical vapor deposition (CCVD). Characterization of the developed catalyst and CNTs were carried out using thermogravimetric analysis (TGA), x-ray diffraction (XRD), specific surface area Brunauer-Emmett-Teller (BET), Fourier-transform infrared spectroscopy (FTIR), high-resolution scanning electron microscopy (HRSEM)/energy dispersive x-ray spectroscopy (EDS) and high-resolution transmission electron microscopy (HRTEM)/selected area electron diffraction (SAED). The BET and TGA analysis indicated that the Fe-Ni-Co/Al_2O_3 catalyst has a high surface area 288.84 $m^2 \cdot g^{-1}$ and is thermally stable. The FTIR of the developed catalyst shows notable functional group with presence of unbound water. The HRSEM of the catalyst revealed agglomerated, homogeneous and porous particles while the HRSEM/HRTEM of the produced CNTs gave the formation of long strand of multiwalled carbon nanotubes (MWCNTs), and homogeneous crystalline fringe like structure with irregular diameter. EDS revealed the dominance of carbon in the elemental composition. XRD/SAED patterns of the catalyst suggest high dispersion of the metallic particles in the catalyst mixture while that of the CNTs confirmed that the produced MWCNTs were highly graphitized and crystalline in nature with little structural defects. The anti-bacteria activity of the produced MWCNTs on *Klebsiella pneumoneae*, *Escherichia coli*, and *Pseudomonas aeruginosa* was also carried out. It was observed that the produced MWCNTs have an inhibitory property on bacteria; *Escherichia coli* and *Klebsiella pneumoneae* from zero day (6.5×10^4 and 7.3×10^3 cfu $\cdot g^{-1}$) through to twelfth day (Nil count) respectively. It has no effect on *Pseudomonas aeruginosa* with too numerous to count at zero-sixth day, but a breakdown in its growth at ninth-twelfth day ($2.0 \times 10^3 \div 1.5 \times 10$ cfu $\cdot g^{-1}$). This study implied that MWCNTs with varying diameter and well-ordered nano-structure can be produced from Fe-Ni-Co/Al_2O_3 catalyst via CCVD method, and it can be recommended that the MWCNTs can be used to treat infected media contaminated with *Klebsiella pneumoneae, Escherichia coli*, and *Pseudomonas aeruginosa.*

1. Introduction

Bacterial infections have been a growth limiting factor on the health of humans. Infections such as urinary tract infections (UTIs) are ones of the frequent infections which are primarily caused by *Escherichia coli*, Klebsiella species, Staphylococcus species, proteus species and Pseudomonas species [1]. *Escherichia coli* (*E. coli*) bacteria usually stay in the guts of living things. Although some species of *E. coli* are mild and needed for a healthy digestion, nevertheless, selected *E. coli* stream are pathogenic, leading to either diarrhoea, or other form of illness outside of the intestinal tract. Major means of transmission of *E. coli* is through contaminated food, water, amongst others. *Klebsiella pneumoneae* is one of the major bacteria causing pneumoneae in human. It also causes stomach constipation and gastric ulcer. *Pseudomonas aeruginosa* is a known adaptable pathogen which causes fatal infections. The challenge is that it possesses distinctive resistance to antibiotics which thereby leads to high rates of diseases and deaths [2]. To mitigate such menace in human health, several materials have been identified to possess high inhibitory properties to the growth and reduction of microbial infection in human. Such materials include silver, copper, gold and carbon nanoparticles [3, 4].

Carbon nanotubes (CNTs) such as pristine CNTs have antimicrobial properties on microorganisms including bacteria such as *Micrococcus lysodeikticus* [5], Streptococcus mutants [6], *E. coli* [7, 8], *Salmonella* [9], and bacteria endospores [10], protozoa species such as *Tetrahymena pyriformis* [11]. The morphological structure of bacteria is altered after incubation with the suspension of CNTs. The cytotoxic characteristic of CNTs helps in improving the microbial inhibition because CNTs simultaneously remove and deactivate pathogens [4, 7, 8]. Thin fibrous nature of CNTs invades the cell surface of bacteria, which abruptly interrupt the intracellular metabolic series and consequently, the internal constituents are distorted [7]. The morphology of carbon nanotubes and its dispersivity nature are identified to cause the cytotoxic characteristics [9].

Moreover, when using catalytic chemical vapour deposition (CCVD) method, CNTs development involves impregnation of catalyst on substrate as support [12]. Transition metals such as Fe, Ni, Co, Mo, Pd are usually loaded in single, binary or ternary form on support such as alumina, silica, titania, $CaCO_3$ and zeolites, to prepare catalyst materials for CNTs production [13]. In this study, multiwall carbon nanotubes (MWCNTs) were produced through CCVD techniques through the use of the developed trimetallic Fe-Ni-Co/Al_2O_3. The MWCNTs were later tested for their anti-bacteria activity against some selected bacteria; *E. coli*, *K. pneumoneae* and *P. aeruginosa*.

2. Methodology

2.1. Material

Chemicals utilized in this study are of analytical grade with percentage purity in the ranges of 98%–99.99%. Chemicals used include nickel (II) trioxonitrate hexahydrate, cobalt (II)
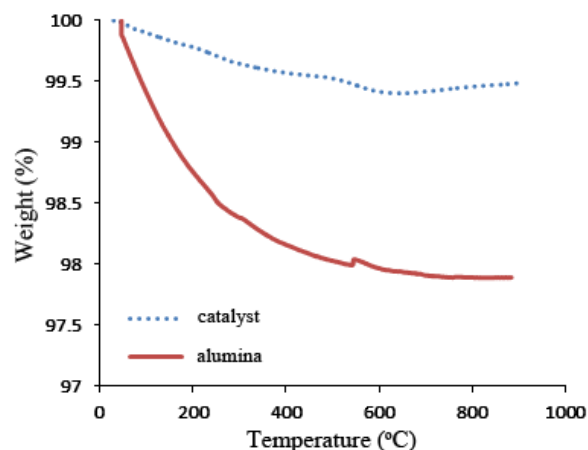

Figure 1. Thermal behaviour of the prepared trimetallic catalyst (Fe-Ni-Co/Al_2O_3) and raw alumina.

trioxonitrate hexahydrate, iron (III) trioxonitrate nonahydrate, alumina, and concentrated tetraoxosulphate (VI) acid were obtained from Sigma Aldrich. Argon and ethylene were gotten from British Oxygen Company (BOC Gases Nigeria Plc, Lagos).

2.1.1. Preparation of Fe-Ni-Co/Al_2O_3 *trimetallic catalyst.*
In the preparation of Fe-Ni-Co/Al_2O_3, wet impregnation method was utilized with equal weight percentage of Fe, Ni and Co supported on Al_2O_3. About 4.55 g of Fe$(NO_3)_3 \cdot 9H_2O$, 3.27 g of Ni$(NO_3)_2 \cdot 6H_2O$ and 3.28 g of Co$(NO_3)_2 \cdot 6H_2O$ mixed in 50 cm³ of distilled water. The resulting mixture was added to 10 g of Al_2O_3 and aged at room temperature for 30 min. The expected slurry was dried at temperature of 110 °C in an oven for 7 h and cooled to room temperature. The powder obtained was ground and calcined at 400 °C for 16 h. The final product, Fe-Ni-Co/Al_2O_3 catalyst was sieved through 150 μm.

2.1.2. Production of carbon nanotubes.
Carbon nanotubes were synthesized by the catalytic disintegration of C_2H_2 gas in a CVD reactor on Fe-Ni-Co/Al_2O_3 catalyst. 1 g of the Fe-Ni-Co/Al_2O_3 catalyst was placed in the ceramic boat, which was inserted in the horizontal quartz tube of the CVD furnace and heating was done at 10 °C min⁻¹. As the temperature increased and carrier gas (argon) was allowed to run over Fe-Ni-Co/Al_2O_3 catalyst at a flow rate of 30 ml min⁻¹ to cap the system off air. On reaching the temperature of 750 °C, the argon gas was flown at rate of 200 ml min⁻¹ followed by the introduction of acetylene gas flown at rate of 100 ml min⁻¹ for 45 min. At the end of the reaction, the product was weighed to determine the quantity of CNTs produced.

2.1.3. Antimicrobial activities of CNTs.
Microbial wastewater was simulated through non-synthetic media which were used and they are Nutrient Agar and MacConkey Agar, prepared according to manufacturer' specification: 28 g and 58 g of powdered Nutrient Agar and MacConkey Agar were differently dissolved in 1000 cm³ distilled water respectively. The two media were autoclaved (sterilized) at 121 °C and pressure of 1.5 N m⁻² for 15 min. 0.005 g of purified MWCNTs was weighed into conical flask, 2 g of nutrient broth (serve as

Adv. Nat. Sci.: Nanosci. Nanotechnol. **9** (2018) 025008

S O Ibrahim *et al*
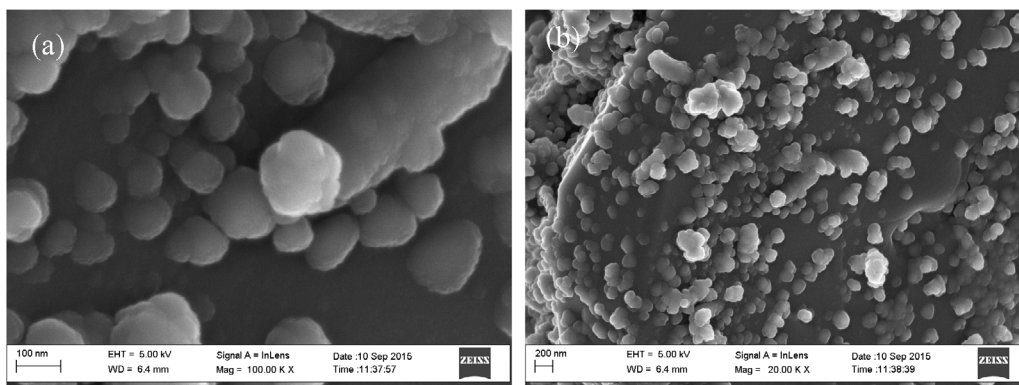
Figure 2. HRSEM images of the developed Fe-Ni-Co/Al$_2$O$_3$ catalyst.

nutrient for microbial growth) with 100 cm^3 of distilled were added into the flask. The substrate contained in the flask was sterilized with autoclave, 0.1 cm^3 of the culture (24 h old bacteria culture of *E. coli*, *P. aeruginosa*, and *K. pneumoneae*) was inoculated into the substrate and mixed. There was serial dilution of substrate-culture and inoculated into the Nutrient Agar and MacConkey Agar inside an empty sterile petri dish accordingly (initial cultivation of micro-organism) and was allow to solidify. The solidify media with inoculum was incubated at 37 °C for 24 h and the original substrate with bacteria at same temperature, after 24 h the colonies were counted and recorded from initial (zero day). The substrate was left in the incubator for 72 h (third day) and inoculated again into the media, the mixture was then incubated at same temperature, and the colonies were counted and recorded. This was repeated at 144 h (sixth day), 216 h (ninth day) and 288 h (twelfth day).

3. Results and discussion

This study deals with synthesis and application of carbon nanotubes as anti-bacteria substrate against the growth of microbes. The prepared Fe-Ni-Co/Al$_2$O$_3$ catalyst and the produced CNTs were characterized to determine their capability for CNTs production and antimicrobial properties of CNTs respectively. It is expected that the materials (catalyst and CNTs) produced must have high surface area and porosity, and be thermally stable. The MWCNTs were synthesized via CCVD techniques using the developed trimetallic Fe-Ni-Co/Al$_2$O$_3$ catalyst.

3.1. TGA of Fe-Ni-Co/Al$_2$O$_3$

Figure 1 depicts the thermal stability of the alumina template and the bimetallic supported catalyst. The TGA examines the behaviours of materials as a function of percentage weight and derivative weight against temperature [14].

At 800 °C, the percentage weight difference retain in the catalyst increase by 1.621% compared to the Al$_2$O$_3$ support. This is as a result of the presence of transition metals (Fe, Co and Ni) impregnated on Al$_2$O$_3$ in the Fe-Ni-Co/Al$_2$O$_3$ composition raised the thermal behaviour of the alumina for CNTs growth. This result implies improvement of the thermal

stability of the prepared trimetallic Fe-Ni-Co/Al$_2$O$_3$ catalyst compared to the raw alumina.

3.2. HRSEM/EDS analysis of Fe-Ni-Co/Al$_2$O$_3$

High resolution scanning electron microscope was employed in the determination of the surface morphology of the synthesized trimetallic Fe-Ni-Co/Al$_2$O$_3$. The micrograph is presented in figure 2.

It was observed on the HRSEM micrographs that the catalyst particles are agglomerated with dense homogeneously distribution on the support substrate at its surface. Also reveals on the synthesized catalyst was pores indicated by the arrows, an indication of its enhancement in the flow of the acetylene to the reactive site of the Fe-Ni-Co/Al$_2$O$_3$ catalyst during the growth of CNTs. This was reflected in the BET result of an enhancement in the surface area and pore size of the prepared Fe-Ni-Co/Al$_2$O$_3$ catalyst. The elemental composition of the developed Fe-Ni-Co/Al$_2$O$_3$ catalyst was examined via the EDS as shown in figure 3.

The EDS analysis confirm the presence of Fe, Ni, Co, O, Al, Br and C. Though, the presence of Br in the catalyst could be attributed to the method adopted while preparing the sample for the HRSEM analysis. The presence of Fe, Co, Ni and Br indicate the ability of those elements to exist at two varied energy level of either low or high when they occur at oxide state [15].

3.3. Brunauer-Emmet-Teller analysis of Fe-Ni-Co/Al$_2$O$_3$ catalyst

Brunauer-Emmet-Teller (BET) or N$_2$ adsorption was used to determine the porosity and surface area of the Fe-Ni-Co/Al$_2$O$_3$ catalyst. The results gotten shows that the surface area of the Fe-Ni-Co/Al$_2$O$_3$ catalyst was 288.24 m$^2 \cdot$ g^{-1} compared to the raw alumina (support) which is 2.95 m$^2 \cdot$ g^{-1}. The possible reason for the surface area enhancement may be linked to the reaction of the metallic hydrated salts into their different oxides during the wet impregnation process. This shows that more openings were created on the Al$_2$O$_3$ substrate for easy penetration of Fe-Ni-Co particles. The pore size and pore volume of the Fe-Ni-Co/Al$_2$O$_3$ catalyst obtained were 3.021 nm and 0.090 cm$^3 \cdot$ g^{-1} respectively, depicting the
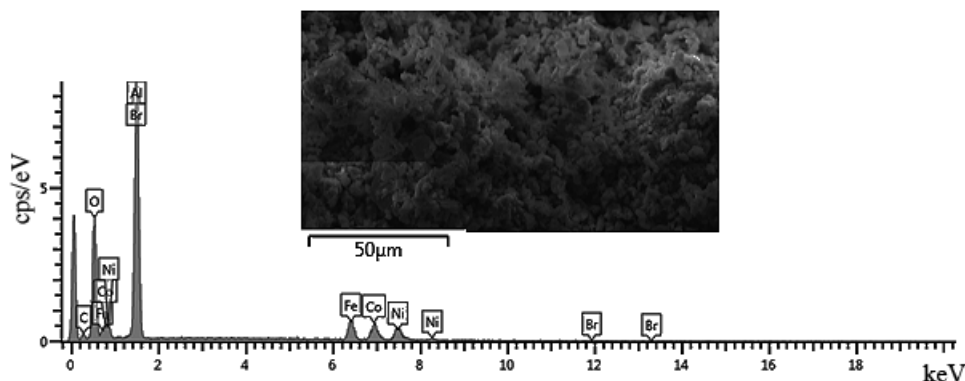
Adv. Nat. Sci.: Nanosci. Nanotechnol. **9** (2018) 025008

S O Ibrahim *et al*

Figure 3. EDS analysis of Fe-Ni-Co/Al$_2$O$_3$ catalyst.
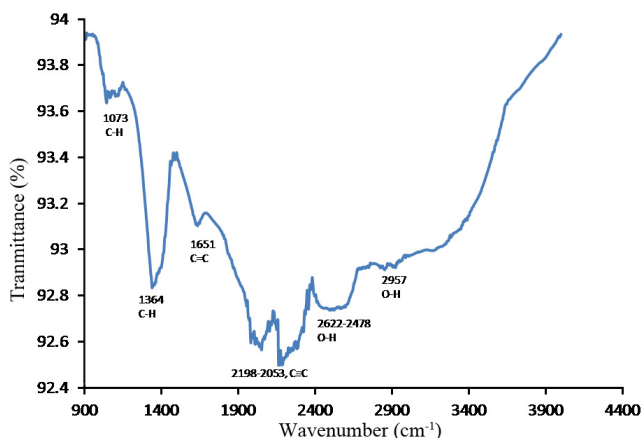
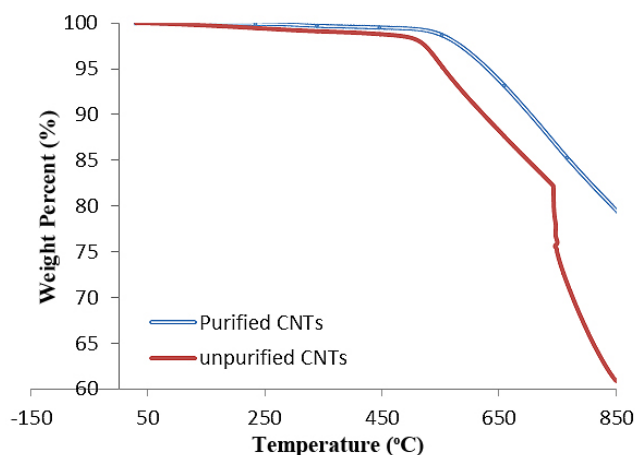**Figure 4.** FTIR spectrum of the developed trimetallic Fe-Ni-Co/Al$_2$O$_3$ catalyst.
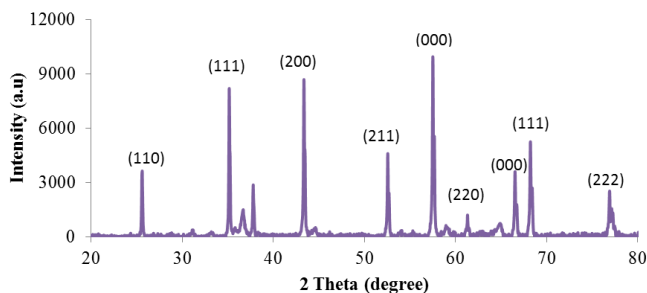

Figure 5. XRD pattern of Fe-Ni-Co/Al$_2$O$_3$ catalyst.

activeness and effectiveness of the prepared catalyst for its suitability for production of CNTs using CCVD technique.

3.4. FTIR analysis of Fe-Ni-Co/Al$_2$O$_3$ catalyst

The functional group present on the developed Fe-Ni-Co/Al$_2$O$_3$ catalyst was examined with the aid of FTIR. The result of the analysis is shown in figure 4.

The spectral as depicted in figure 4 shows the varied functional group present in the trimetallic catalyst developed. The presence of water molecule is manifest with the occurrence of broad peak at $2622 - 2478 \, \text{cm}^{-1}$ and peak at $2957 \, \text{cm}^{-1}$ which characterize the presence of $O - H$ group (attributed to the unbound water molecule at post-calcination of the catalyst material). Other peaks observed are at 2198, 2053, 1651
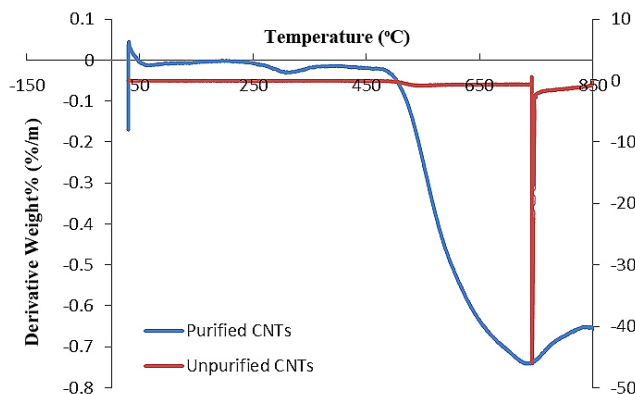

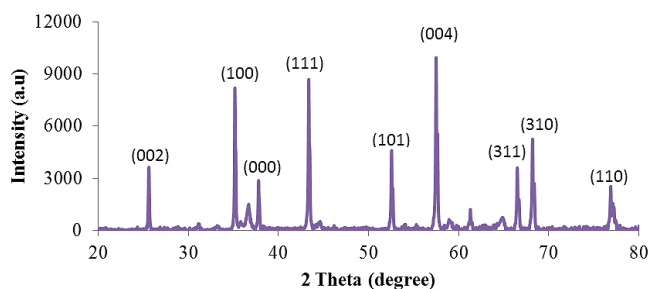**Figure 6.** TGA curves of as-synthesized and purified CNTs.

Figure 7. DTG curves of as-synthesized and purified CNTs.

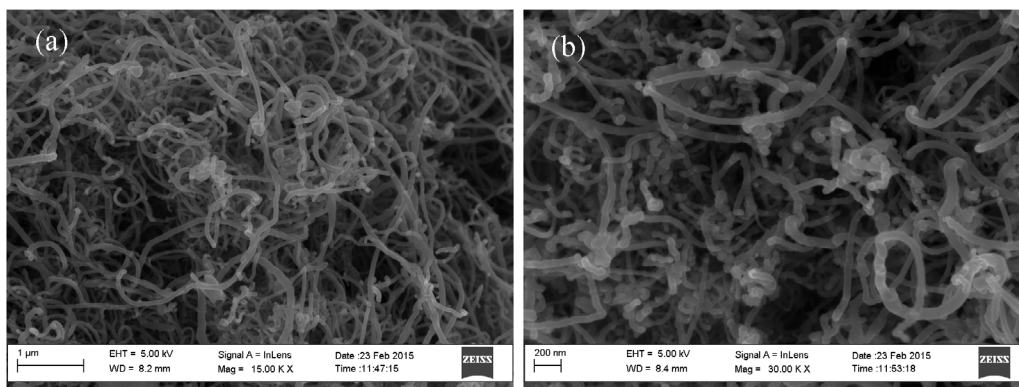**Figure 8.** XRD pattern of synthesized CNTs.

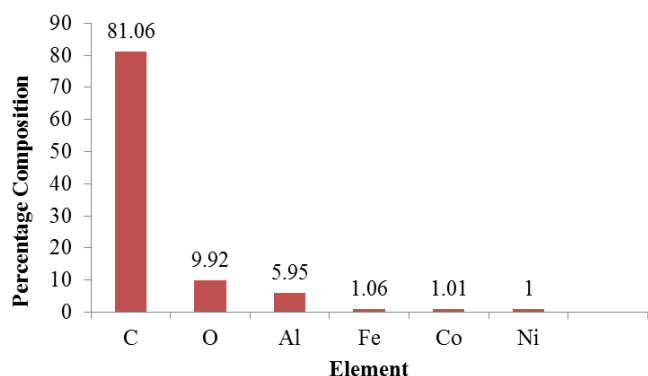**Figure 9.** HRSEM images of the developed CNTs.

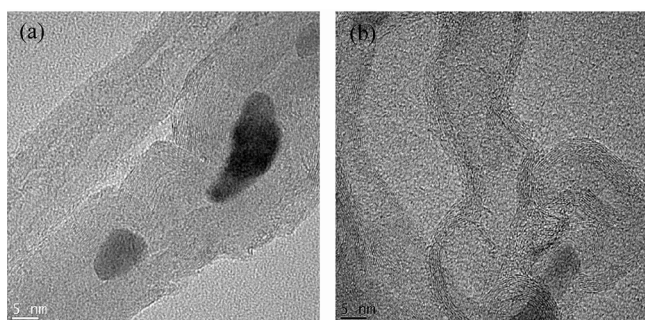**Figure 10.** EDS analysis of the developed CNTs showing different elements.

Figure 11. HRTEM Images of (a) as-synthesized and (b) purified CNTs.

and $1364 \, \mathrm{cm}^{-1}$ which can be assigned to the presence of complex oxides and stretching vibration at $1073 \, \mathrm{cm}^{-1}$ for ferrites. This finding agrees closely with the report of Abdulkareem *et al* [15].

3.5. *XRD pattern of* Fe-Ni-Co/Al$_2$O$_3$ *catalyst*

Figure 5 shows the XRD pattern of the Fe-Ni-Co/Al$_2$O$_3$ catalyst.

The main noticeable peaks at the diffraction angle are: 26.3, 35.6, 37.5, 43.9, 52.1, 57.5, 61.3, 66.1, 68.6 and 77.9° with reflection plane of (110), (111), (111), (200), (211),
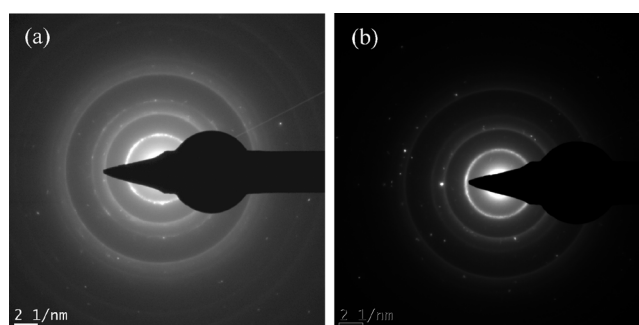

Figure 12. SAED of (a) as-synthesized and (b) purified MWCNTs.

Table 1. Anti-bacteria activity of P-CNTs on selected bacteria.

Bacteria (cfu g^{-1})	Zero day (initial)	Third day	Sixth day	Ninth day	Twelfth day
K. pneumoneae	6.5×10^4	0	0	0	0
P. aeruginosa	TNM	TNM	TNM	2.0×10^3	1.5×10
E. coli	7.3×10^3	0	0	0	0

Cfu = Colony forming unit, TNM = too numerous to count.

(000), (220), (000), (111) and (222) respectively. The characteristic peak at 2θ of 37.5, 43.9 and 57.5 are associated to CoFe$_2$O$_4$ [16]. The peaks at 37.5 and 52.1° are possible reflection peak for NiFe$_2$O$_3$. While the peak at 66.1° signifies the likely occurrence of a metallic oxide complex; NiCoFe$_2$O$_3$ with no observable reflection plane (000). Also in figure 5, Fe, Ni or Co (individually) were not detected, which suggest high dispersion of the metallic particles on the support Al$_2$O$_3$ in the Fe-Ni-Co/Al$_2$O$_3$ catalyst. However, it was revealed in the XRD pattern, the presence of alumina metallic oxides complex peaks further confirms the reaction between the metals Fe-Ni-Co catalyst particles and Al$_2$O$_3$.

3.6. *TGA/DTA of CNTs*

Both the as-synthesized (un-purified) and purified CNTs were characterized using TGA and differential thermal gravity (DTG) to determine their thermal stability as shown in figures 6 and 7.

Table 2. Anti-bacteria activity of Ag-NPs on selected bacteria.

Bacteria	AgNPs [27]	AgNPs [22]	PsAgNPs [30]	AgNPs [29]	AgNPs [26]	LG-AgNPs [24]	AgNPs [25]	AgNPs [23]
P. aeruginosa	—	—	Strong inhibition (83%)	MIC at 10 μg ml^{-1}	—	—	—	MIC at 45 mg l^{-1}
E. coli	MIC at 5 μg ml^{-1}	MIC at 9.4 μg ml^{-1}	Strong inhibition (83.63%)	MIC at 10 μg ml^{-1}	MIC at 100 mg l^{-1}	MIC at 31.25-62.5 μg ml^{-1}	MIC at 7.8 μg ml^{-1}	MIC at 35 mg l^{-1}

As revealed in figure 6, the TGA results showed that the percentage purity of the synthesized CNTs was 79.55% with lesser volatile organic constituents compare to as-synthesized CNTs. The peak temperature, T_P (optimum temperature of degradation) of both the purified and as- synthesized CNTs were obtained to be 738.67 °C and 743.44°C, respectively. The noticeable high T_p in un-purified CNTs is linked to the presence of impurities that emanate in the catalyst used in the CNTs production [17, 18]. After the purification process, the impurities (amorphous carbon and metals oxides) were removed and reduced, which aids to lower the peak temperature of the purified carbon nanotubes. Temperature at which 50% of the material degraded, T50 were also determined to be greater than 850 °C which is an indication of high thermal stability of the CNTs. Hence the CNTs produced with trimetallic catalyst, Fe-Ni-Co/Al$_2$O$_3$ is thermally stable.

3.7. XRD analysis of CNTs

The fully characterized Fe-Ni-Co/Al$_2$O$_3$ catalyst developed was channeled towards the synthesis of high crystalline and purity carbon nanotubes in a catalytic vapour deposition (CVD) equipment. Figure 8 shows the XRD result of the synthesized multi-walled carbon nanotubes.

This show that carbon in the MWCNTs synthesized possesses two phases in the bulk material. According to figure 8, three major phases which represent carbon, alumina, and metallic oxide complex were noticed. The diffraction peaks at $2\theta = 25°$ corresponding to a crystal plane (002) belongs to graphitized MWCNTs. Maccallini *et al* [19] reported that the occurrence of the plane (002) implies multi-layer coverage of the crystalline carbon on the Fe-Ni-Co/Al$_2$O$_3$ nanoparticles. And also, a visibly distinct peak was observed at 43.3° for the produced CNTs. The peak observed at $2\theta = 35.5°$ showed a mixed phase formed from the wet impregnation reaction between the Al$_2$O$_3$ and the metallic oxides (Fe$_2$O$_3$ and CoO). The peaks at $2\theta = 68°$ and 76° approximately correspond to planes (310) and (110) which are typical peaks given to the NiO and Co$_3$O$_4$, respectively.

3.8. HRSEM/EDS of CNTs

The surface morphology of the synthesized CNTs was investigated using HRSEM. Figure 9 shows the formation of long-coiled irregular tube-like nature of the multiwalled carbon nanotubes.

Figure 9 further shows the formation of long strand of multi-walled carbon nanotubes (MWCNTs), and densely

homogeneous of tube-like structure with irregular diameter. The variation in the diameter of the produced MWCNTs could be traced to the characteristics diameter of the developed catalyst material. The presence of densely populated strand of MWCNTs is related to the complete carbon nucleation process during the thermal cracking process. Therefore, the developed Fe-Ni-Co/Al$_2$O$_3$ catalyst shows high performance properties to the enhancement of the acetylene cracking in the CVD technique. To gain more understanding about the elemental constituent of the developed MWCNTs, the material was analysed via EDS technique. The results of the analysis are shown in figure 10. The result as depicted shows several elements as contained in the MWCNTs developed. The elements include C, Al, O, with Fe, Co and Ni and their respective percentage composition (figure 10).

Figure 10 shows the presence of C, O, Al, Fe, Co and Ni with percentage composition of 81.06%, 9.92%, 5.95%, 1.06%, 1.01% and 1% respectively. The highest percentage of carbon pesent in the bulk material shows the presence of graphitized carbon while oxygen indicates the presence of the oxides of the metallic composition in the form of impurities.

3.9. HRTEM/SAED of CNTs

The morphologies and the microstructure of the as-synthesized and purified CNTs were examined using HRTEM and the results are shown in figures 11(a) and (b).

The HRTEM image of as-synthesized CNTs (figure 11(a)) shows that the CNTs synthesized are tube/rope-like structure MWCNTs, with the presence of encapsulated metals within the walls of the CNTs. The purified MWCNTs (figure 11(b)) shows the graphitic nature of the MWCNTs, removal of metallic impurities due to oxidative purification, which was further confirm by the EDS result of figure 10. To study the phases present in the prepared MWCNTs, it was further evaluated via the SAED pattern also collected from the HRTEM analysis (figure 12).

The SAED pattern of as-synthesized MWCNTs in figure 12(a) showed some levels of crystal plane but not as the purified MWCNTs in figure 12(b), which revealed the presence of two broad crystal plane corresponding to (002) and (100) respectively. This result agrees with the report of Cong *et al* [20]. The SAED patterns of all samples confirmed the graphitic nature of MWCNTs especially the innermost ring which is due to the usual strongest reflection plane (002) of graphite. As presented in figure 12, the occurrence of the sharp rings at reciprocal lattice spacing (1/d) of 2.9, 4.8,

Adv. Nat. Sci.: Nanosci. Nanotechnol. **9** (2018) 025008

S O Ibrahim *et al*

5.7 and 8.5 nm^{-1} is in accordance with those reported for graphite.

3.10. Anti-bacteria activity of MWCNTs

The well-characterized MWCNTs were tested for its antibacterial properties and the effects of the MWCNTs are presented in table 1.

From table 1, it was shown that the selected infectious bacteria were treated using the P-CNTs. It was observed that the MWCNTs has bactericidal effects on *K. pneumoneae* and *E. coli* because the number of cells of the bacteria were reduced through the days (72 ÷ 288 h), showing no multiplicity effect thereby inhibiting the growth, which is in accordance with the works of Shahzadi *et al* [21] and Ebrahiminezhad *et al* [22]. And when comparing with the results in table 2 of minimum inhibition concentration (MIC) of Ag-NPs and its composite, it is confirmable with the earlier reports of anti-bacteria activity against *E. coli* which exhibited high inhibitory property [23–27]. However, as revealed in table 1, P-CNTs have no effect on *Pseudomonas aeurigonosa*. This phenomenon was similar to the report of Qilin *et al* [28], who reported that there was no significant inhibition to tested *P. aeruginosa* by Au-NPs. This is because *P. aeurigonosa* is a terrible bacterium that resists the action of most of the antibiotics because it has ability to secret β-lactamase that destroys most of the antibiotics in human body. The behaviour is in contrast with high inhibition of *P. aeruginosa* by Ag-NPs and Ps-Ag-NPs composite as reported by Kumari *et al* [29] and Golvindappa *et al* [30] respectively. Nevertheless, the inhibition potential of *P. aeruginosa* was broken and decreases by the produced MWCNTs (216 and 288 h) with a significant difference from too numerous to count to the least count of 15 cfu · g^{-1}. Therefore it is appreciable that MWCNTs as a substrate can inhibit (stop) the growth of these bacteria. From the fore going on this experiment, it can be recommended that the MWCNTs can be used to treat infected media contaminated with *K. pneumoneae*, *E. coli*, and *P. aeruginosa.*

4. Conclusions

This work revealed that trimetallic Fe-Ni-Co/Al$_2$O$_3$ catalyst and MWCNTs were produced by utilizing wet impregnation and CCVD method respectively. The prepared Fe-Ni-Co/Al$_2$O$_3$ catalyst shows its effectiveness and efficiency in the development of tube-like structure MWCNTs in a CCVD. Characterization of the developed trimetallic Fe-Ni-Co/Al$_2$O$_3$ catalyst and CNTs were carried out using TGA, XRD, BET, FTIR, HRSEM/EDS and HRTEM/SAED to confirm their thermal stability, crystallinity, surface area, attached functional groups and morphology/elemental composition respectively. The anti-bacteria activity of the produced MWCNTs on *K. pneumoneae*, *E. coli*, and *P. aeruginosa* showed that the produced MWCNTs have an inhibitory property on the selected bacteria. Therefore, the MWCNTs can be used to treat infected media contaminated with *K. pneumoneae*, *E. coli*, and *P. aeruginosa.*

References

[1] Hamza S and Abdulhadi S K 2016 *Am. J. Biomed. Life Sci.* **4** 11
[2] Amadi E, Uzoaru P, Orji I, Nwaziri A and Iroha I 2008 *Int. J. Infect. Dis.* **7** 1
[3] Ruparelia J P, Chatterjee A K, Duttagupta S P and Mukherji S 2008 *Acta Biomater.* **4** 707
[4] Kang S, Pinault M, Pfefferle L D and Elimelech M 2007 *Langmuir* **23** 8670
[5] Nepal D, Balasubramanian S, Simonian A L and Davis V A 2008 *Nano Lett.* **8** 1896
[6] Akasaka T and Watari F 2009 *Acta Biomater.* **5** 607
[7] Kang S, Herzberg M, Rodrigues D F and Elimelech M 2008 *Langmuir* **24** 6409
[8] Kang S, Mauter S M and Elimelech M 2008 *Environ. Sci. Technol.* **42** 7528
[9] Arias L R and Yang L 2009 *Langmuir* **25** 3003
[10] Krishna V, Pumprueg S, Lee S H, Zhao J, Sigmund W and Koopman B 2005 *Trans IChemE* B **83** 393
[11] Zhu Y, Ran T, Li Y, Guo J and Li W 2006 *Nanotechnology* **17** 4668
[12] Chang L 2015 *J. Ind. Catal.* **23** 45
[13] Motchelaho A M M 2011 *PhD Thesis* submitted to the faculty of engineering and the built environment University of the Witwatersrand, Johannesburg
[14] Okpalugo T I T, Papakonstantinou P, Murphy H, Mclaughlin J and Brown N M D 2005 *Carbon* **4** 2951
[15] Abdulkareem A S, Kariim I, Bankole M T, Tijani J O, Abodunrin T F and Olu S C 2017 *Arab. J. Sci. Eng.* **42** 4365
[16] Naseri M G, Saion E B, Ahangar H A, Shaari A H and Hashim M 2010 *J. Nanomater.* **2010** 1
[17] Ebbensen T, Ajayan A and Tanigaki K 1994 *Nature* **367** 519
[18] Eftehari A, Jafarkhani P and Moztarzadeh F 2005 *Carbon* **44** 1298
[19] Maccallini E, Tsoufis T, Policicchio A, La Rosa S, Caruso T, Chiarello G, Colavita E, Formoso V, Gournis D and Agostino R G 2010 *Carbon* **48** 3434
[20] Cong Y, Li X, Qin Y, Dong Z, Yuan G, Cui Z and Lai X 2011 *Appl. Catal.* B **107** 128
[21] Shahzadi S, Noshin Z, Saira R, Rehana S, Jawad N and Shahzad N 2016 *Nanomaterials* **6** 1
[22] Ebrahiminezhad A, Bagheri M, Taghizadeh S M, Berenjian A and Ghasemi Y 2016 *Adv. Nat. Sci.* **7** 015018
[23] Mittal J, Jain R and Sharma M M 2017 *Adv. Nat. Sci.* **8** 025011
[24] Ajayi E and Afolayan A 2017 *Adv. Nat. Sci.* **8** 015017
[25] Erjaee H, Rajaian H and Nazifi S 2017 *Adv. Nat. Sci.* **8** 025004
[26] Rao B and Tang R C 2017 *Adv. Nat. Sci.* **8** 015014
[27] Kumar V A, Uchida T, Mizuki T, Nakajima Y, Katsube Y, Hanajiri T and Maekawa T 2016 *Adv. Nat. Sci.* **7** 015002
[28] Qilin Y, Jianrong L, Yueqi Z, Yufan W, Lu L and Mingchun L 2016 *Sci. Rep.* **6** 1
[29] Kumari R M, Thapa N, Gupta N, Kumar A and Nimesh S 2016 *Adv. Nat. Sci.* **7** 045009
[30] Govindappa M, Farheen H, Chandrappa C P, Channabasava R, Rai R V and Raghavendra V B 2016 *Adv. Nat. Sci.* **7** 035014